

Contribution from the Department of Chemistry, Emory University, Atlanta, Georgia 30322,
and Dipartimento di Scienze Chimiche, Università di Trieste, 34127 Trieste, Italy

Structures, NMR Spectra, and Ligand-Exchange Properties of Costa-Type Organocobalt B₁₂ Models with N-Donor Ligands

Wallace O. Parker, Jr.,[†] Ennio Zangrando,[‡] Nevenka Bresciani-Pahor,[‡] Lucio Randaccio,^{*‡}
and Luigi G. Marzilli^{*‡}

Received January 27, 1986

In this report, we describe the first extensive characterization of ligand-exchange rates and ¹H NMR spectral properties of the Costa-type organocobalt B₁₂ model system [LCo((DO)(DOH)pn)CH₃]X, where L = N-donor ligand, X = ClO₄ or PF₆, and (DO)(DOH)pn = N²,N^{2'}-propanediylbis(2,3-butanedione 2-imine 3-oxime). The three-dimensional structures of [PhNH₂Co((DO)(DOH)pn)R]PF₆, with R = CH₃ (I) and R = CH₂CO₂CH₃ (II), were determined. Crystallographic details follow. I: C₁₈H₂₉CoF₆N₅O₂P, P2₁/n, a = 13.912 (3) Å, b = 20.996 (3) Å, c = 8.048 (1) Å, β = 93.38 (2)°, D(calcd) = 1.56 g cm⁻³, Z = 4, R = 0.054 for 3640 independent reflections. II: C₂₀H₃₁CoF₆N₅O₄P, P1, a = 8.052 (3) Å, b = 8.077 (2) Å, c = 10.699 (2) Å, α = 71.30 (2)°, β = 74.05 (2)°, γ = 85.95 (2)°, D(calcd) = 1.60 g cm⁻³, Z = 1, R = 0.035 for 3008 independent reflections. The only other complexes of the type [LCo((DO)(DOH)pn)R]X (L = N-donor ligand) that have been structurally characterized contain L = py (pyridine). In these compounds, the orientation of the py ligand is rotated by 90° relative to the O-H...O moiety in comparison to related cobaloximes, (py)Co(DH)₂R (where DH = monoanion of dimethylglyoxime). In contrast, the aniline ligand, PhNH₂, occupies a similar orientation in the two series of B₁₂ models. The axial Co-N bond distances, 2.147 (3) (I) and 2.126 (3) (II) Å, are not significantly different from those expected from comparisons to cobaloxime structures. However, the rate of PhNH₂ dissociation is actually smaller than that in cobaloximes. These data and an analysis of ¹H and ¹³C NMR spectral shifts suggest that the Co center in [LCo((DO)(DOH)pn)R]X compounds is more electrophilic than that in analogous LCo(DH)₂R species. In contrast, the magnetic anisotropy of the Co((DO)(DOH)pn)R⁺ moiety appears to be greater than that of the Co(DH)₂R moiety. These results, in conjunction with previous findings, support the view that the Costa-type compounds are not significantly different from cobaloximes as models for B₁₂.

Introduction

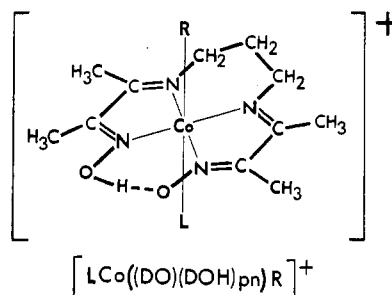
We have previously listed reasons for studying in more detail the coordination chemistry of B₁₂ model compounds.¹⁻⁵ Many questions remain about the coordination number and structural features of coenzyme B₁₂ both when it is in solution and when it is incorporated into B₁₂-dependent enzymes.⁵ In particular, the Costa-type model (see scheme below)⁶⁻¹⁵ has not been extensively studied in terms of its coordination chemistry, but it exhibits many interesting properties, which have led Finke's group to examine a related system in detail as a B₁₂ model.¹⁶⁻²²

In this report, we describe a continuation of our studies on this system.^{14,15,22} One unifying theme of these previous studies has been to draw direct comparisons with the cobaloxime model systems LCo(DH)₂R (DH = monoanion of dimethylglyoxime). As can be seen from the Chart I, the planarity of the equatorial (DO)(DOH)pn ligand is disrupted by the pucker of the propylene bridge. In a previous study, which focused on a comparison of pyridine complexes in the two B₁₂ model series, we discovered that the relative orientations of the pyridine (py) ligand were different with respect to the O-H...O group(s).¹⁴ This finding was attributed to the steric interaction of the py with the propylene bridge, which led to a rotation of 90° by the py ligand with respect to its orientation in the cobaloxime series. We felt that structural data on complexes with an N-donor ligand that has a smaller effective bulk in the vicinity of the Co would permit a more direct comparison between the model systems. Complexes with aniline (PhNH₂) met this requirement. In addition, for complexes with several other N-donor ligands (2-aminopyridine (2NH₂py), 2-amino-6-methylpyridine (2NH₂6MePy), 4-cyanopyridine (4CNpy), 3,5-lutidine (3,5LUT), 4-(dimethylamino)pyridine (4Me₂NPy), quinoline (QUIN), 1,5,6-trimethylbenzimidazole (Me₃Bzm), 1-methylimidazole (NMeImd), 1-acetylimidazole (AcImd), 1,2-dimethylimidazole (1,2Me₂Imd), thiazole (THIAZ), aminoacetaldehyde dimethyl acetal (DEA), tert-butylamine (tBuNH₂), p-anisidine (MeOPhNH₂), N,N-dimethyl-1,4-phenylenediamine (Me₂NPhNH₂), and NH₃), we have compared complexes in the two series to assess factors influencing L dissociation rates and ¹H NMR chemical shifts.

Experimental Section

Reagents. PhNH₂ was purchased from Fisher and distilled under vacuum before use. Me₃Bzm was prepared by a procedure similar to that

Chart I



given for 1-ethyl-5,6-dimethylbenzimidazole.²³ Ethyldiphenylphosphine was from Strem. All other ligands and reagents were obtained from

- (1) Bresciani-Pahor, N.; Forcolin, M.; Marzilli, L. G.; Randaccio, L.; Summers, M. F.; Toscano, P. J. *Coord. Chem. Rev.* **1985**, *63*, 1.
- (2) Toscano, P. J.; Marzilli, L. G. *Prog. Inorg. Chem.* **1984**, *31*, 105.
- (3) Summers, M. F.; Toscano, P. J.; Bresciani-Pahor, N.; Nardin, G.; Randaccio, L.; Marzilli, L. G. *J. Am. Chem. Soc.* **1983**, *105*, 6259.
- (4) Summers, M. F.; Marzilli, L. G.; Bresciani-Pahor, N.; Randaccio, L. *J. Am. Chem. Soc.* **1984**, *106*, 4478.
- (5) Marzilli, L. G.; Summers, M. F.; Bresciani-Pahor, N.; Zangrando, E.; Charland, J.-P.; Randaccio, L. *J. Am. Chem. Soc.* **1985**, *107*, 6880.
- (6) Costa, G.; Mestroni, G.; Savorgnani, E. *Inorg. Chim. Acta* **1969**, *3*, 323.
- (7) Pellizer, G.; Tauszik, G. R.; Costa, G. *J. Chem. Soc., Dalton Trans.* **1973**, 317.
- (8) Bigotto, A.; Costa, G.; Mestroni, G.; Pellizer, G.; Puxeddu, A.; Reisenhofer, E.; Stefani, L.; Tauzher, G. *Inorg. Chem.* **1970**, *4*, 41.
- (9) Costa, G.; Mestroni, G.; Licari, T.; Mestroni, E. *Inorg. Nucl. Chem. Lett.* **1969**, *5*, 561.
- (10) Pellizer, G.; Tauszik, G. R.; Tauzher, G.; Costa, G. *Inorg. Chim. Acta* **1973**, *7*, 60.
- (11) Fox, J. P.; Banninger, R.; Proffitt, R. T.; Ingraham, L. L. *Inorg. Chem.* **1972**, *11*, 2379.
- (12) Guschi, R. J.; Brown, T. L. *Inorg. Chem.* **1974**, *13*, 959.
- (13) Costa, G. *Pure Appl. Chem.* **1972**, *30*, 335.
- (14) Parker, W. O., Jr.; Bresciani-Pahor, N.; Zangrando, E.; Randaccio, L.; Marzilli, L. G. *Inorg. Chem.* **1985**, *24*, 3908.
- (15) Parker, W. O., Jr.; Bresciani-Pahor, N.; Zangrando, E.; Randaccio, L.; Marzilli, L. G. *Inorg. Chem.* **1986**, *25*, 1303.
- (16) Finke, R. G.; Schiraldi, D. A.; Mayer, B. J. *Coord. Chem. Rev.* **1984**, *54*, 1.
- (17) Finke, R. G.; Schiraldi, D. A. *J. Am. Chem. Soc.* **1983**, *105*, 7605 and references therein.
- (18) Finke, R. G.; McKenna, W. P.; Schiraldi, D. A.; Smith, B. L.; Pierpoint, C. J. *J. Am. Chem. Soc.* **1983**, *105*, 7592.
- (19) Finke, R. G.; Smith, B. L.; Mayer, B. J.; Molinero, A. A. *Inorg. Chem.* **1983**, *22*, 3677.

[†] Emory University.

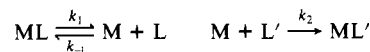
[‡] Università di Trieste.

Aldrich. Elemental analyses (C, H, N; supplementary table) performed by Atlantic Microlabs, Atlanta, GA, were satisfactory for all complexes used in kinetic studies.

Rate Measurements. Ligand-substitution reactions were monitored spectrophotometrically with a Perkin-Elmer Lambda 3B instrument equipped with a 3600 Data Station for the slower reactions ($k_{\text{obsd}} < 0.05 \text{ s}^{-1}$) or a Durrum-Gibson D-110 stopped-flow spectrophotometer for the faster reactions. Both instruments were equipped with thermostated cell compartments ($25.0 \pm 0.04 \text{ }^\circ\text{C}$). Visible spectra of several (DO)-(DOH)pn complexes in methylene chloride were recorded and then compared with the visible spectra of the same solutions after addition of a calculated excess (in most cases 100:1) of entering ligand (L') and allowing sufficient time for the reactions to reach completion (verified by a similar ^1H NMR experiment).

Trimethyl phosphite was used as an entering ligand except in two cases ($\text{L} = \text{DEA}$, $\text{L}' = \text{NMeImd}$; $\text{L} = \text{NMeImd}$, $\text{L}' = \text{P}(\text{OMe})_2\text{Ph}$). Suitable wavelengths for following the exchange reactions were in the range 440–480 nm for the complexes (0.0005–0.001 M) studied. Absorbance changes over the first 3 half-lives were used in the calculations of the rate constants with the final absorbance taken at 8 half-lives. At least three data sets were collected for each complex.

Data Analysis. The rate constants are defined as follows:



where $\text{M} = \text{Co}(\text{DO})(\text{DOH})\text{pnR}$ and L' is a suitable entering ligand. The experimental absorbance vs. time rate data were treated with the standard integrated expression for a first-order process by using a linear least-squares computer program.

^1H NMR Spectroscopy. ^1H NMR spectra were recorded on a Nicolet NB-360 spectrometer operating at 361.08 MHz and contained 16K data points with a spectral range of 9500 Hz. All chemical shifts are relative to internal Me_4Si with CDCl_3 as solvent. If solubility permitted, ca. 3 mg of complex was dissolved in 0.5 mL of CDCl_3 .

^1D NOE experiments were performed on the NMeImd , $1,2\text{Me}_2\text{Imd}$, and Me_3Bzm ligands, both free and complexes as $\text{LCo}(\text{DH})_2\text{CH}_3$ and $[\text{LCo}(\text{DO})(\text{DOH})\text{pnCH}_3]\text{ClO}_4$. Partial saturation of the N1-CH_3 signal with the ^1H decoupler during the off-acquisition delay enhanced the signals of nearby protons (e.g. H2 and H5 for NMeImd , H2 and C2- CH_3 for $1,2\text{Me}_2\text{Imd}$, and H2 and H7 for Me_3Bzm). The off-resonance spectra (^1H decoupler set ca. 360 Hz away from the N1-CH_3 signal) and the on-resonance spectra were alternately collected (4 scans each, 32–46 scans total) and subtracted to give the difference spectra. Signals that were not enhanced in the difference spectra were assigned to H4 since these protons are too distant (greater than 5 Å) from the N1-CH_3 protons to be affected by NOE.²⁴

Preparation of $[\text{LCo}(\text{DO})(\text{DOH})\text{pnCH}_3]\text{ClO}_4$ Complexes. To avoid cleavage of the Co–C bond, all compounds with Co–C bonds were handled with minimal exposure to light and were not subjected to temperatures above 35 $^\circ\text{C}$.

$[\text{H}_2\text{OC}(\text{DO})(\text{DOH})\text{pnCH}_3]\text{ClO}_4$ was prepared according to Costa's method b⁶ with the following equivalents of reactants: CH_3I , 3; NaBH_4 , 1.5; NaClO_4 , ca. 5.

$[\text{H}_2\text{OC}(\text{DO})(\text{DOH})\text{pnCH}_3]\text{PF}_6$ was prepared as reported earlier.¹⁵

$[\text{LCo}(\text{DO})(\text{DOH})\text{pnCH}_3]\text{ClO}_4$ ($\text{L} = \text{py}$, 4CNpy , $4\text{Me}_2\text{Npy}$, $3,5\text{LUT}$, THIAZ , NMeImd , AcImd , $1,2\text{Me}_2\text{Imd}$, tBuNH_2 , $\text{Me}_2\text{NPhNH}_2$). A mixture of $[\text{H}_2\text{OC}(\text{DO})(\text{DOH})\text{pnCH}_3]\text{ClO}_4$ (200 mg, 0.46 mmol) in CH_2Cl_2 (5–10 mL) was treated with L (1.2 equiv) and stirred until a clear solution resulted. The solution was filtered and treated with petroleum ether until it became cloudy. Acetone was used to dissolve any oil that formed. Precipitation of the product was induced when the solution was scratched and cooled (0 $^\circ\text{C}$). The product was collected and washed with petroleum ether or diethyl ether. For $\text{L} = \text{Me}_2\text{NPhNH}_2$, the precipitate was recrystallized twice from CH_2Cl_2 /petroleum ether to remove a dark green compound. For $\text{L} = 4\text{CNpy}$, an oily precipitate was obtained. This oil was dissolved in acetone (10 mL) and treated with more 4CNpy (0.5 equiv). The product precipitated from the cooled solution (5 $^\circ\text{C}$, 24 h). Yields: $\text{L} = \text{py}$, 133 mg (50%); $\text{L} = 4\text{CNpy}$, 155

Table I. Crystallographic Data for Compounds I and II at 18 $^\circ\text{C}$

	I	II
formula	$\text{CoO}_2\text{N}_5\text{C}_{18}\text{H}_{29}\text{PF}_6$	$\text{CoO}_4\text{N}_5\text{C}_{20}\text{H}_{31}\text{PF}_6$
M_r	551.4	609.5
a , Å	13.912 (3)	8.052 (3)
b , Å	20.996 (3)	8.077 (2)
c , Å	8.048 (1)	10.699 (2)
α , deg		71.30 (2)
β , deg	93.38 (2)	74.05 (2)
γ , deg		85.95 (2)
$D(\text{measd})$, g cm^{-3}	1.55	1.58
$D(\text{calcd})$, g cm^{-3}	1.56	1.60
Z	4	1
space group	$P2_1/n$	$P1$
μ , cm^{-1}	8.7	8.2
transmission: max, min	0.99, 0.95	1.00, 0.97
cryst dimens, cm^3	$0.02 \times 0.03 \times 0.05$	$0.04 \times 0.03 \times 0.02$
no. of reflns measd	6217	3224
no. of indep reflns	3640	3008
($I > 3\sigma(I)$)		
max 2θ , ^a deg	56	56
R	0.054	0.035
R_w	0.073	0.045

^a Mo $K\alpha$ radiation; $\lambda = 0.71073 \text{ \AA}$.

mg (62%); $\text{L} = 4\text{Me}_2\text{Npy}$, 210 mg (82%); $\text{L} = 3,5\text{LUT}$, 80 mg (33%); $\text{L} = \text{THIAZ}$, 200 mg (74%); $\text{L} = \text{NMeImd}$, 198 mg (80%); $\text{L} = \text{AcImd}$, 150 mg (62%); $\text{L} = 1,2\text{Me}_2\text{Imd}$, 210 mg (86%); $\text{L} = \text{tBuNH}_2$, 148 mg (66%); $\text{L} = \text{Me}_2\text{NPhNH}_2$, 35 mg (13%).

$[\text{LCo}(\text{DO})(\text{DOH})\text{pnCH}_3]\text{ClO}_4$ ($\text{L} = \text{DEA}$, MeOPhNH_2). These complexes were prepared as above (for $\text{L} = \text{py}$) except a $\text{CHCl}_3/\text{Et}_2\text{O}$ solvent system was used. A crystalline product formed from a clear solution (1:2 $\text{CHCl}_3/\text{Et}_2\text{O}$) left standing for 1 h at 23 $^\circ\text{C}$. Yields: $\text{L} = \text{DEA}$, 130 mg (55%); $\text{L} = \text{MeOPhNH}_2$, 158 mg (63%).

$[\text{Me}_3\text{BzmCo}(\text{DO})(\text{DOH})\text{pnCH}_3]\text{ClO}_4$. A solution of Me_3Bzm (89 mg, 0.56 mmol) in methanol (15 mL) was added to $[\text{H}_2\text{OC}(\text{DO})(\text{DOH})\text{pnCH}_3]\text{ClO}_4$ (200 mg, 0.46 mmol). The mixture was stirred and warmed until the solid dissolved, and then it was filtered. The large red crystals, which formed on letting this solution stand for 3 days at 23 $^\circ\text{C}$, were collected.

$[\text{LCo}(\text{DO})(\text{DOH})\text{pnCH}_3]\text{PF}_6$ ($\text{L} = \text{QUIN}$, Me_3Bzm). These complexes were obtained as for $\text{L} = \text{py}$ except $[\text{H}_2\text{OC}(\text{DO})(\text{DOH})\text{pn-CH}_3]\text{PF}_6$ was the starting material. Yields: $\text{L} = \text{QUIN}$, 78 mg (29%); $\text{L} = \text{Me}_3\text{Bzm}$, 240 mg (83%).

$[\text{PhNH}_2\text{Co}(\text{DO})(\text{DOH})\text{pnCH}_3]\text{ClO}_4$. A solution of $[\text{H}_2\text{OC}(\text{DO})(\text{DOH})\text{pnCH}_3]\text{ClO}_4$ (230 mg, 0.5 mmol) in H_2O (50 mL) was treated with PhNH_2 (0.5 mL, 5.5 mmol). The mixture was stirred until an orange suspension formed (ca. 15 min). A bright orange powder was collected and washed with Et_2O . Yield: 190 mg (70%).

$[\text{PhNH}_2\text{Co}(\text{DO})(\text{DOH})\text{pnCH}_3]\text{PF}_6$. This complex was obtained as a powdered precipitate from the above procedure for $\text{L} = \text{QUIN}$. X-ray quality crystals were obtained from a methanol/ H_2O (2:1) solution of the powder left standing for ca. 2 days at 23 $^\circ\text{C}$.

$[\text{PhNH}_2\text{Co}(\text{DO})(\text{DOH})\text{pnCH}_2\text{CO}_2\text{CH}_3]\text{PF}_6$. A solution of $[\text{H}_2\text{OC}(\text{DO})(\text{DOH})\text{pnCH}_2\text{CO}_2\text{CH}_3]\text{PF}_6$ (250 mg, 0.5 mmol) in methanol (30 mL) was treated with PhNH_2 (0.1 mL, 1.1 mmol). X-ray quality crystals were obtained from this solution after 3 days at 23 $^\circ\text{C}$.

X-ray Methods. Crystals of $[\text{PhNH}_2\text{Co}(\text{DO})(\text{DOH})\text{pnR}]\text{PF}_6$, where $\text{R} = \text{CH}_3$ (I) and $\text{R} = \text{CH}_2\text{CO}_2\text{CH}_3$ (II), were red rectangular prisms obtained as detailed above. Cell dimensions determined from Weissenberg and precession photographs were refined on a CAD4 Enraf Nonius single-crystal diffractometer (Table I). Intensities of three check reflections, measured about every 100 reflections, did not show any systematic decay throughout the data collection. Intensities having $I > 3\sigma(I)$ were corrected for Lorentz and polarization factors and for anomalous dispersion, but not for extinction. No correction for absorption was included because of the small size of the crystals used and the small values of the absorption coefficients.

Solution and Refinement of Structures. The structures of I and II were solved by conventional Patterson and Fourier methods and then refined by full-matrix least-squares methods to final R values of 0.054 and 0.035, respectively. The contribution of the hydrogen atoms, located at calculated positions except for those on the disordered C6, was held constant ($B = 5 \text{ \AA}^2$) in both structures. The final weighting scheme was $w = 1/(\sigma(F)^2 + (pF)^2 + q)$ where $p = 0.03$ and 0.02 and $q = 3.0$ and 1.0 for I and II, respectively. The weighting scheme was chosen so as to maintain $w(|F_o| - |F_c|)^2$ essentially constant over all ranges of $|F_o|$ and $(\sin \theta)/\lambda$. For compound (II) the final refinement was carried out for

- Finke, R. G.; Smith, B. L.; McKenna, W. A.; Christian, P. A. *Inorg. Chem.* **1981**, *20*, 687.
- Elliot, C. M.; Hershenhart, E.; Finke, R. G.; Smith, B. L. *J. Am. Chem. Soc.* **1981**, *103*, 5558.
- Marzilli, L. G.; Bresciani-Pahor, N.; Randaccio, L.; Zangrando, E.; Myers, S. A.; Finke, R. G. *Inorg. Chim. Acta* **1985**, *107*, 139.
- Simonav, A. M.; Pozharskii, A. E.; Marianovskii, V. M. *Indian J. Chem.* **1967**, *5*, 81.
- Noggle, J. H.; Schirmer, R. E. *The Nuclear Overhauser Effect*; Academic: New York, 1971.

Table II. Atomic Positional Parameters and Their Estimated Standard Deviations for Compound I

atom	x	y	z	atom	x	y	z
Co	0.20810 (4)	0.07623 (3)	-0.00978 (7)	C9	0.1583 (3)	-0.0257 (2)	-0.2025 (6)
O1	0.2897 (3)	0.0813 (2)	0.3198 (4)	C10	0.1869 (3)	-0.0522 (2)	-0.0398 (6)
O2	0.2396 (3)	-0.0243 (2)	0.2224 (4)	C11	0.1900 (5)	-0.1214 (3)	0.0025 (9)
N1	0.2614 (3)	0.1149 (2)	0.1855 (4)	C12	0.0782 (3)	0.0837 (2)	0.0798 (7)
N2	0.2111 (3)	-0.0080 (2)	0.0666 (5)	C13	0.3810 (3)	0.0120 (2)	-0.1776 (5)
N3	0.1578 (2)	0.0360 (2)	-0.2084 (4)	C14	0.4054 (3)	-0.0445 (2)	-0.0988 (6)
N4	0.2022 (3)	0.1630 (2)	-0.0824 (5)	C15	0.4289 (4)	-0.0966 (3)	-0.1936 (8)
N5	0.3536 (2)	0.0660 (2)	-0.0807 (5)	C16	0.4269 (4)	-0.0926 (3)	-0.3637 (8)
C1	0.3269 (5)	0.2111 (3)	0.3180 (8)	C17	0.4024 (4)	-0.0369 (3)	-0.4401 (6)
C2	0.2766 (3)	0.1755 (2)	0.1815 (6)	C18	0.3797 (3)	0.0164 (2)	-0.3481 (6)
C3	0.2388 (3)	0.2034 (2)	0.0236 (6)	P	-0.0019 (1)	0.2747 (6)	0.2844 (2)
C4	0.2462 (4)	0.2738 (2)	-0.0007 (8)	F1	0.0386 (5)	0.3431 (2)	0.2752 (7)
C5	0.1588 (4)	0.1829 (3)	-0.2443 (7)	F2	0.0991 (3)	0.2555 (4)	0.3494 (7)
C6	0.0864 (6)	0.1352 (4)	-0.320 (1)	F3	-0.0382 (4)	0.2072 (2)	0.3000 (7)
C6*	0.175 (1)	0.1368 (8)	-0.377 (2)	F4	-0.1022 (3)	0.2970 (4)	0.2224 (6)
C7	0.1270 (4)	0.0711 (3)	-0.3591 (6)	F5	0.0258 (3)	0.2619 (2)	0.0982 (4)
C8	0.1344 (5)	-0.0683 (3)	-0.3463 (8)	F6	-0.0344 (3)	0.2889 (2)	0.4661 (4)

Table III. Atomic Positional Parameters and Their Estimated Standard Deviations for Compound II

atom	x	y	z	atom	x	y	z
Co	0.300	0.300	0.300	C9	0.3887 (5)	0.5809 (6)	0.0679 (4)
O1	0.1513 (4)	-0.0240 (3)	0.3449 (3)	C10	0.3254 (5)	0.4453 (6)	0.0275 (4)
O2	0.2195 (4)	0.1679 (4)	0.1073 (3)	C11	0.3094 (7)	0.4692 (8)	-0.1122 (4)
O3	0.7352 (4)	0.1988 (5)	0.3726 (4)	C12	0.5351 (5)	0.1883 (5)	0.2471 (4)
O4	0.5799 (4)	-0.0419 (4)	0.4349 (3)	C13	0.6268 (4)	0.1196 (5)	0.3549 (4)
N1	0.2072 (4)	0.0769 (4)	0.4000 (3)	C14	0.6707 (7)	-0.1179 (8)	0.5396 (6)
N2	0.2813 (4)	0.3014 (4)	0.1277 (3)	C15	-0.0103 (4)	0.5446 (4)	0.2411 (4)
N3	0.3901 (4)	0.5298 (4)	0.1947 (3)	C16	-0.0163 (5)	0.7102 (5)	0.2531 (5)
N4	0.3232 (4)	0.2934 (4)	0.4744 (3)	C17	-0.0633 (6)	0.8514 (6)	0.1540 (6)
N5	0.0433 (4)	0.3975 (4)	0.3405 (3)	C18	-0.1065 (6)	0.8255 (7)	0.0447 (6)
C1	0.1197 (7)	-0.1469 (6)	0.6251 (6)	C19	-0.1036 (6)	0.6582 (7)	0.0351 (5)
C2	0.1978 (5)	0.0274 (5)	0.5292 (4)	C20	-0.0563 (5)	0.5180 (5)	0.1329 (4)
C3	0.2692 (5)	0.1542 (5)	0.5719 (4)	P	-0.1873 (2)	0.3575 (2)	-0.2483 (1)
C4	0.2804 (7)	0.1128 (8)	0.7158 (5)	F1	-0.2588 (5)	0.5247 (5)	-0.2043 (4)
C5	0.3970 (5)	0.4385 (6)	0.4991 (4)	F2	-0.3397 (7)	0.2449 (8)	-0.1370 (7)
C6	0.5160 (8)	0.5576 (9)	0.3734 (7)	F3	-0.1129 (5)	0.1938 (5)	-0.2955 (5)
C6*	0.372 (1)	0.610 (1)	0.4053 (9)	F4	-0.0331 (6)	0.4643 (6)	-0.3602 (6)
C7	0.4502 (6)	0.6464 (5)	0.2548 (5)	F5	-0.3062 (5)	0.4036 (7)	-0.3466 (5)
C8	0.4370 (8)	0.7516 (7)	-0.0298 (6)	F6	-0.0721 (6)	0.3098 (7)	-0.1456 (5)

both chiralities, obtaining final *R* indexes of 0.035 and 0.040, respectively, with no significant differences in molecular geometry. Atomic scattering factors were those given in ref 25. All calculations were carried out by using the SDP-CAD4 programs on a PDP11-44 computer. Final positional parameters are given in Tables II and III. Hydrogen atom coordinates, anisotropic thermal parameters, and final calculated and observed structure factors are available as supplementary material.

Results

Synthetic Methods. Complexes of the type [LCo((DO)(DOH)pn)CH₃]X have been isolated previously with the following N-donor ligands: L = Imd, Bzm;⁶ NH₂R (R = H, Me, Et, *n*-Bu);¹⁰ NCMe, NMe₃, CF₃Imd, 3Fpy;¹² py;^{11,14} 3Xpy and 4Xpy (X = Me, CN, NH₂).¹¹ A closely related Me₃Bzm compound has been isolated.²⁰ Two of the complexes reported in this work, [LCo((DO)(DOH)pn)CH₃]⁺ (L = 2NH₂py and QUIN), could not be isolated as ClO₄⁻ salts.

Rate Measurements. The ligand-exchange rate constants (*k*₁) were determined for 16 [LCo((DO)(DOH)pn)CH₃]X salts in the noncoordinating solvent CH₂Cl₂ and are listed in Table IV with those for the analogous LCo(DH)₂CH₃ compounds. Concentrations of the cobalt complexes used in the rate studies of this work (1–2 mM) were lower than in previous determinations (10–20 mM).^{14,26,27}

Ligand-exchange rates were found to be independent of [L'] (L' = P(OMe)₃, concentrations varied from 10 to at least 100 times [Co]) for the following [LCo((DO)(DOH)pn)CH₃]X

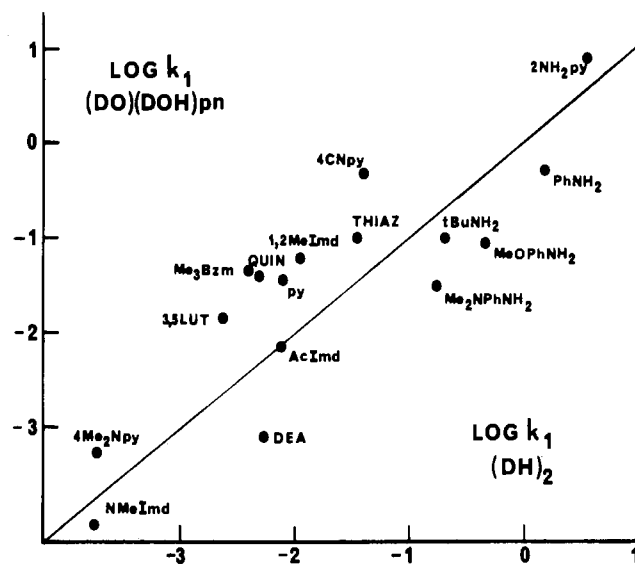


Figure 1. Plot of $\log k_1$ (s⁻¹) for LCo(DH)₂CH₃ vs. $\log k_1$ (s⁻¹) for [LCo((DO)(DOH)pn)CH₃]ClO₄; solvent, CH₂Cl₂; T, 25 °C.

complexes: L = 4CNpy, tBuNH₂, 3,5SLUT, 2NH₂py. Therefore, as found previously for [pyCo((DO)(DOH)pn)R]ClO₄ complexes¹⁴ and [PPh₃Co((DO)(DOH)pn)CH₃]ClO₄,¹⁵ the rate expression is first order in complex concentration and independent of entering ligand concentration as expected for an S_N1 LIM reaction.

The exchange rates for PhNH₂ and MeOPhNH₂ were found to increase with [L'] (P(OMe)₃, PEtPh₂) at low [L']. However,

(25) International Tables for X-ray Crystallography; Kynoch: Birmingham, England, 1974; Vol. IV.

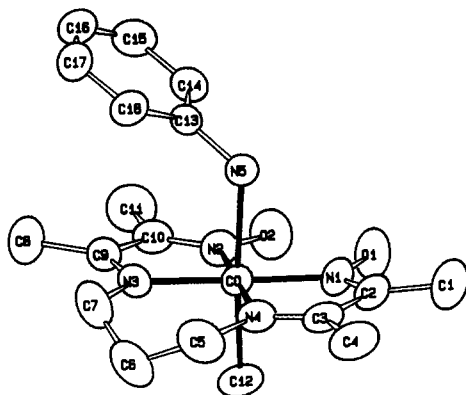
(26) Bayo, F., unpublished results.

(27) Charland, J.-P., unpublished results.

Table IV. First-Order Rate Constants for L Exchange of $\text{LCo}(\text{chel})\text{CH}_3$ in CH_2Cl_2 at 25 °C

L	k_1, s^{-1}	
	$[\text{LCo}((\text{DO})(\text{DOH})\text{pn})\text{CH}_3]\text{ClO}_4$	$\text{LCo}(\text{DH})_2\text{CH}_3^e$
$2\text{NH}_2\text{py}$	7.7 ± 0.1^a	3.5 ± 0.1
PhNH_2	$(5.0 \pm 0.1) \times 10^{-1}^b$	1.51 ± 0.04
4CNpy	$(4.9 \pm 0.2) \times 10^{-1}$	$(4.1 \pm 0.3) \times 10^{-2}$
$t\text{BuNH}_2$	$(1.03 \pm 0.01) \times 10^{-1}$	$(2.05 \pm 0.03) \times 10^{-1}^f$
THIAZ	$(9.9 \pm 0.3) \times 10^{-2}$	$(3.5 \pm 0.1) \times 10^{-2}$
MeOPhNH_2	$(9.0 \pm 0.2) \times 10^{-2}^b$	$(4.7 \pm 0.1) \times 10^{-1}^f$
$1,2\text{Me}_2\text{Imd}$	$(5.9 \pm 0.3) \times 10^{-2}$	$(1.1 \pm 0.1) \times 10^{-2}$
Me_3Bzm	$(4.34 \pm 0.06) \times 10^{-2}^c$	$(4.19 \pm 0.04) \times 10^{-3}^g$
QUIN	$(4.0 \pm 0.1) \times 10^{-2}^a$	$(4.95 \pm 0.01) \times 10^{-3}^g$
py	$(3.4 \pm 0.1) \times 10^{-2}$	$(8.0 \pm 0.8) \times 10^{-3}$
$\text{Me}_2\text{NPhNH}_2$	$(3.0 \pm 0.1) \times 10^{-2}$	$(1.7 \pm 0.1) \times 10^{-1}^h$
3,5LUT	$(1.5 \pm 0.1) \times 10^{-2}^d$	$(2.36 \pm 0.06) \times 10^{-3}^h$
AcImd	$(7.3 \pm 0.1) \times 10^{-3}$	$(7.5 \pm 0.1) \times 10^{-3}^h$
DEA	$(7.7 \pm 0.1) \times 10^{-4}$	$(5.4 \pm 0.2) \times 10^{-3}^f$
$4\text{Me}_2\text{Npy}$	$(5.6 \pm 0.1) \times 10^{-4}$	$(1.89 \pm 0.05) \times 10^{-4}^i$
NMeImd	$(9.9 \pm 0.1) \times 10^{-5}$	$(1.78 \pm 0.02) \times 10^{-4}^i$

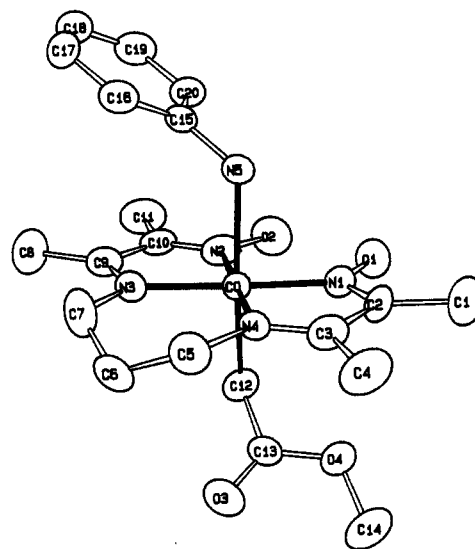
^aRate constant given is for the PF_6^- salt. ^bLimiting rate constant. ^c $k_1 = (4.0 \pm 0.1) \times 10^{-2} \text{ s}^{-1}$ for the PF_6^- salt. ^d $k_1 = (1.6 \pm 0.1) \times 10^{-2} \text{ s}^{-1}$ with PEtPh_2 as the entering ligand. $k_1 = (2.10 \pm 0.02) \times 10^{-2} \text{ s}^{-1}$ for the PF_6^- salt with $\text{P}(\text{OMe})_3$ as the entering ligand. $[(3,5\text{LUT})\text{Co}((\text{DO})(\text{DOH})\text{pn})\text{CH}_3]\text{PF}_6$ was obtained by the procedure for L = QUIN and recrystallized from methanol/ H_2O . ^eReference 1 unless indicated otherwise. ^fReference 26. ^gReference 27. ^hThis work. These $(\text{DH})_2$ complexes were prepared from $\text{H}_2\text{OCo}(\text{DH})_2\text{CH}_3^3$ by the same method reported above for $[\text{pyCo}((\text{DO})(\text{DOH})\text{pn})\text{CH}_3]\text{ClO}_4$. Anal. Calcd for L = $\text{Me}_2\text{NPhNH}_2$, $\text{C}_{17}\text{H}_{29}\text{CoN}_6\text{O}_4 \cdot \text{H}_2\text{O}$: C, 44.54; H, 6.82; N, 18.33. Found: C, 44.57; H, 6.83; N, 18.33. Anal. Calcd for L = 3,5LUT, $\text{C}_{16}\text{H}_{26}\text{CoN}_5\text{O}_4 \cdot 1/2\text{H}_2\text{O}$: C, 45.72; H, 6.47; N, 16.66. Found: C, 45.87; H, 6.31; N, 16.72. Anal. Calcd for L = AcImd, $\text{C}_{14}\text{H}_{23}\text{CoN}_6\text{O}_5 \cdot 0.4\text{CH}_2\text{Cl}_2$: C, 38.17; H, 5.29; N, 18.55. Found: C, 37.82; H, 5.11; N, 18.80. ⁱRate constant was redetermined from previously prepared compounds.¹

**Figure 2.** ORTEP drawing (thermal ellipsoid; 50% probability) and labeling scheme for the non-hydrogen atoms of I. Only the C6 atom is reported.

this effect (which is under investigation) was not observed with $\text{L}' = \text{NMeImd}$. For all three L' , essentially the same limiting rate is obtained with $\text{L} = \text{PhNH}_2$ (Table IV). A similar dependence on $[\text{L}']$ was not observed for $\text{PhNH}_2\text{Co}(\text{DH})_2\text{CH}_3$.

A plot of $\log k_1$ for dissociation of L from $\text{LCo}(\text{DH})_2\text{CH}_3$ vs. $\log k_1$ for dissociation of L from $[\text{LCo}((\text{DO})(\text{DOH})\text{pn})\text{CH}_3]\text{X}$ is shown in Figure 1. Ligands found to exchange faster and slower in the $\text{Co}(\text{DO})(\text{DOH})\text{pn}$ system than in the $\text{Co}(\text{DH})_2$ system lie above and below the line in Figure 1, respectively. The line in Figure 1 is the "45° line".

Structural Studies. ORTEP drawings of cations I and II with the atom-numbering scheme are depicted in Figures 2 and 3. In both the compounds, the $(\text{DO})(\text{DOH})\text{pn}$ ligand occupies the four equatorial positions of a distorted octahedron around the Co atom. Selected bond lengths and angles are reported in Tables V and VI. The $\text{Co}(\text{DO})(\text{DOH})\text{pn}$ unit is very similar in both compounds. The four equatorial N atoms are coplanar within ± 0.027

**Figure 3.** ORTEP drawing (thermal ellipsoid; 50% probability) and labeling scheme for the non-hydrogen atoms of II. Only the C6 atom is reported.**Table V.** Selected Bond Lengths (Å) with Estimated Standard Deviations for I and II

	I	II	I	II
Co-N1	1.882 (3)	1.874 (4)	Co-N4	1.913 (3)
Co-N2	1.872 (3)	1.887 (4)	Co-N5	2.147 (3)
Co-N3	1.905 (3)	1.920 (4)	Co-C12	1.991 (4)
				2.038 (4)

Table VI. Selected Bond Angles (deg) for I and II

	I	II
N1-Co-N2	97.7 (2)	97.4 (2)
N1-Co-N3	178.3 (1)	178.4 (2)
N1-Co-N4	81.5 (2)	81.9 (2)
N1-Co-N5	86.2 (1)	87.3 (1)
N1-Co-C12	89.2 (2)	89.2 (2)
N2-Co-N3	81.7 (2)	81.4 (2)
N2-Co-N4	178.2 (1)	178.4 (2)
N2-Co-N5	89.4 (1)	88.9 (1)
N2-Co-C12	87.6 (2)	84.7 (2)
N3-Co-N4	99.2 (2)	99.3 (2)
N3-Co-N5	92.2 (1)	91.6 (1)
N3-Co-C12	92.4 (2)	91.8 (2)
N4-Co-N5	92.2 (1)	92.4 (1)
N4-Co-C12	90.7 (2)	93.9 (2)
N5-Co-C12	174.1 (2)	172.3 (2)
Co-N5-C13	120.4 (2)	
Co-N5-C15		120.8 (3)

(4) (I) and ± 0.021 (3) Å (II) with the cobalt atom in their mean planes.

The two chemically equivalent halves of the equatorial macrocycle, except for C6, are approximately planar. These planes make dihedral angles (vide infra) of -11.3 (I) and -4.6° (II) with the "bending" toward NH_2Ph . The disorder of C6 was interpreted as two orientations of the carbon atom with occupancy factors 0.7 and 0.3 in I and 0.6 and 0.4 in II. Occupancies were fixed on the basis of the respective electron densities of the peaks in the Fourier map. C6 indicates the position of lowest occupancy. The $\text{O}\cdots\text{O}$ distances of the oxime bridges are 2.441 (5) (I) and 2.454 (5) Å (II).

The L-Co-R fragment is characterized by a N-Co-C angle of 174.1 (2) (I) and 172.3 (2)° (II). The Co-N and Co-C distances are 2.147 (3) (I) and 2.126 (3) Å (II) and 1.991 (4) (I) and 2.038 (4) Å (II), respectively. The other bond lengths and angles are in the range usually observed for other complexes of this type.¹⁴

¹H NMR Spectra Signal Assignments. The ¹H NMR chemical shift data for the methyl complexes of the $\text{Co}(\text{DH})_2$ and $\text{Co}(\text{DO})(\text{DOH})\text{pn}$ systems are gathered in Tables VII-IX. The

Table VII. ¹H NMR Chemical Shifts for LCo(DH)₂CH₃ and [LCo((DO)(DOH)pn)CH₃]ClO₄^a Complexes in CDCl₃^b; Equatorial Ligands

L	pK _a ^c	chem shifts								
		Co—CH ₃		O—H...O		O—N=C—CH ₃		C—N=C—CH ₃	N—CH ₂ —C—CH ₂ —N'	
		(DH) ₂	(DO)(DOH)pn	(DH) ₂	(DO)(DOH)pn	(DH) ₂	(DO)(DOH)pn	(DO)(DOH)pn	(DO)(DOH)pn	(DO)(DOH)pn
4CNpy	1.9	0.90	0.90	18.23	18.72	2.13	2.31	2.45	3.73	4.05
THIAZ	2.4	0.86	0.84	18.27	18.84	2.14	2.30	2.43	3.74	4.08
AcImd	3.6	0.83	0.80	18.33	18.84	2.16	2.30	2.42	3.68	4.08
PhNH ₂	4.6	0.81	0.68	18.14	18.77	1.99	2.10	2.18	3.55	3.87
QUIN	4.9	0.87	0.87	18.43	18.94	2.13	2.27	2.39	3.89	4.15
MeOPhNH ₂	5.3	0.78	0.67	18.10	18.77	2.00	2.11	2.21	3.55	3.81
py	5.9	0.83	0.85	18.32	18.80	2.13	2.30	2.45	3.79	4.07
Me ₃ Bzm	6.0 ^d	0.84	0.81	18.63	19.23	2.10	2.29	2.40	3.78	4.13
3,5LUT	6.2	0.77	0.82	18.33	18.83	2.13	2.30	2.44	3.86	4.13
Me ₂ NPhNH ₂	6.6	0.77	0.66	18.15	18.85	1.99	2.10	2.16	3.59	3.85
2NH ₂ py	6.7	e	0.75	e	18.77	e	2.10	2.22	3.63	3.83
NMeImd	7.0	0.74	0.72	18.38	18.90	2.14	2.30	2.42	3.68	4.04
1,2Me ₂ Imd	8.0 ^d	0.74	0.75	18.39	19.00	2.14	2.28	2.41	3.77	3.99
DEA	8.8 ^d	0.69	0.61	18.12	18.77	2.22	2.31	2.42	3.59	4.00
NH ₃	9.2	0.75	0.58	e	18.89	2.22	2.27	2.34	3.46	3.90
4Me ₂ Npy	9.7	0.72	0.71	18.32	18.88	2.13	2.28	2.40	3.78	4.06
tBuNH ₂	10.7	e	0.58	e	19.12	e	2.28	2.43	3.59	4.08

^a Complexes with L = QUIN, 2NH₂py and NH₃ were PF₆⁻ salts. ^b Chemical shifts in ppm relative to internal Me₄Si. ^c Unless indicated otherwise, from: Perrin, D. D. *Dissociation Constants of Organic Bases in Aqueous Solution*; Page Bros. Ltd: Norwich, U. K., 1965. ^d Estimated pK_a. ^e Not observed. Poor solubility in CDCl₃. ^f These methylene protons have ¹H NMR signals consisting of two multiplets. The two methylene protons lying on the L side of the propylene bridge were more downfield in the case of [LCo((DO)(DOH)pn)CH₃]ClO₄ (L = PhNH₂, py, Me₃Bzm) by 1D NOE. ^g ¹H NMR signals from the N—C—CH₂—C—N protons were obscured by the larger O—N=C—CH₃ and C—N=C—CH₃ signals for most of the (DO)(DOH)pn complexes and are not reported.

Table VIII. ¹H NMR Chemical Shifts of Imidazole Ligands and Me₃Bzm and Their LCo(DH)₂CH₃ and [LCo((DO)(DOH)pn)CH₃]ClO₄ Complexes^a

compd	chem shifts			
	N1—CH ₃	H2	H4	H5 or H7
NMeImd	3.68	7.41	7.03	6.87
(DH) ₂	3.64	7.44	6.96	6.78
(DO)(DOH)pn	3.78	7.54	6.43	6.83
1,2Me ₂ Imd	3.52	2.37 ^b	6.87	6.77
(DH) ₂	3.48	2.32 ^b	7.12	6.66
(DO)(DOH)pn	3.53	2.05 ^b	6.24	6.84
AcImd	2.62 ^c	8.15	7.48	7.11
(DH) ₂	2.58 ^c	8.14	7.44	7.09
(DO)(DOH)pn	2.72 ^c	7.89	6.65	7.55
Me ₃ Bzm	3.78	7.74	7.55	7.15
(DH) ₂	3.75	7.95	7.98	7.08
(DO)(DOH)pn	3.92	7.70	7.24	7.15
(DO)(DOH)pn ^d	3.86	7.49	7.19	7.11
(DO)(DOH)pn ^e	3.86	7.47	7.22	7.14
Me ₃ Bzm ^d	3.75	7.71	7.47	7.17
(DH) ₂ ^d	3.75	7.90	7.93	7.13
(DO)(DOH)pn ^{d,e}	3.81	7.29	7.07	7.20

^a Chemical shifts in ppm relative to internal Me₄Si (CDCl₃). ^b CH₃ signal. ^c N1-acetyl resonance. ^d CD₂Cl₂. ^e PF₆⁻ salt.

assignment of the H4 signal of the NMeImd ligand (Table VIII) was determined by the 1D NOE experiment described in the Experimental Section, when a delay of 5 s was used. Assignment of the H4 signal was possible with a 3-s delay for free 1,2Me₂Imd and Me₃Bzm and NMeImd, 1,2Me₂Imd, and Me₃Bzm complexed as LCo(DH)₂CH₃ and [LCo((DO)(DOH)pn)CH₃]ClO₄ in CDCl₃. Of the H2 and H5 (or H7) signals, the more downfield signal was assigned to H2. This assignment was confirmed for [Me₃BzmCo((DO)(DOH)pn)CH₃]ClO₄, since the H2 signal was the only methine proton signal not enhanced upon partial saturation of the signals of the methyls at the C5 and C6 position (Figure 4) in the 1D NOE experiment. In addition, the signal of the proton on C2 between the N's is sharp due to the absence of the unresolved coupling, which broadens the other aromatic CH signals. In the case of [AcImdCo((DO)(DOH)pn)CH₃]ClO₄, partial saturation of the most upfield methine ¹H signal enhanced the 7.55 ppm signal but did not enhance the 7.89 ppm signal. This confirms the assignment of the most downfield signal to H2 for

Table IX. ¹H NMR Chemical Shifts of L and for L in LCo(DH)₂CH₃ and [LCo((DO)(DOH)pn)CH₃]ClO₄; Amine and Pyridine Ligands^a

compd	chem shifts			
	α-H	β-H	CH ₃ or γ-H	NH ₂
PhNH ₂	6.69	7.16	6.76	3.65
(DH) ₂	6.64	7.18	7.05	4.14
(DO)(DOH)pn	6.62	7.16	7.03	4.91
MeOPhNH ₂	6.65	6.75	3.75	3.42
(DH) ₂	6.57	6.70	3.73	4.14
(DO)(DOH)pn	6.53	6.68	3.72	4.80
Me ₂ NPhNH ₂	6.67 ^b		2.82	3.35
(DH) ₂	6.52 ^b		2.85	4.00
(DO)(DOH)pn	6.50 ^b		2.85	4.70
DEA	2.80	4.30	3.40	~1.2
(DH) ₂	2.36	4.23	3.31	1.96
(DO)(DOH)pn	2.15	4.52	3.38	2.65
py	8.61	7.29	7.68	
(DH) ₂	8.61	7.33	7.73	
(DO)(DOH)pn	8.03	7.56	7.80	
4CNpy	8.82	7.54		
(DH) ₂	8.85	7.59		
(DO)(DOH)pn	8.24	7.81		
Me ₂ Npy	8.22	6.49	3.00	
(DH) ₂	8.08	6.42	2.98	
(DO)(DOH)pn	7.47	6.64	3.00	

^a Chemical shifts in ppm relative to internal Me₄Si (CDCl₃). ^b Center of multiplet. ¹H NMR resonances from excess Me₂NPhNH₂ in the presence of [Me₂NPhNH₂Co((DO)(DOH)pn)CH₃]ClO₄ or [H₂OCo((DO)(DOH)pn)CH₃]ClO₄ are almost completely broadened.

this complex. Assignment of the H4 signal was made by analogy with chemical shift trends for the other imidazole ligands (Table VIII).

The α-H and β-H signals were assigned for coordinated MeOPhNH₂ in both systems by partial saturation of the NH₂ signal. In both cases, the β-H signal is downfield from the α-H signal (Table IX).

The most extensive 1D NOE studies were performed on the [LCo((DO)(DOH)pn)CH₃]ClO₄ (L = PhNH₂, py, Me₃Bzm) complexes. For all three complexes the propylene N—CH₂ protons give rise to two multiplets separated by ca. 0.3 ppm (Table VII). In each case, partial saturation of the downfield multiplet caused enhancement of the signal from the nearest L proton (α-H or H2).

Table X. Comparisons of Relevant Geometric Parameters for (DO)(DOH)pn and (DH)₂ Complexes^a

compd	Co-C, Å	Co-N, Å	N-Co-C, deg	α, deg	d, Å	k, s ⁻¹
[PhNH ₂ Co((DO)(DOH)pn)CH ₃]PF ₆ (I)	1.991 (4)	2.147 (3)	174.1 (2)	-11.3	0.0	(5.0 ± 0.1) × 10 ⁻¹ ^e
PhNH ₂ Co(DH) ₂ CH ₃ ^b	1.992 (2)	2.129 (4)	178.19 (7)	+3.5	0.04	1.51 ± 0.4
[pyCo((DO)(DOH)pn)CH ₃]PF ₆ ^c	2.003 (3)	2.106 (3)	178.9 (1)	+6.9	0.07	(3.4 ± 0.1) × 10 ⁻²
pyCo(DH) ₂ CH ₃ ^d	1.998 (5)	2.068 (3)	178.0 (2)	+3.2	0.04	(8.0 ± 0.8) × 10 ⁻³
[PhNH ₂ Co((DO)(DOH)pn)CH ₂ CO ₂ CH ₃]PF ₆ (II)	2.038 (4)	2.126 (3)	172.3 (2)	-4.6	0.0	
pyCo(DH) ₂ CH ₂ CO ₂ CH ₃ ^d	2.024 (6)	2.039 (6)	175.6 (3)			

^a Positive values of α and d indicate that the bending of the equatorial ligand is toward the alkyl group and that the displacement of Co out of the N4 equatorial donor set is toward L. ^b Reference 28. ^c Reference 14. ^d Reference 1. ^e Limiting L exchange rate with high [L']. This rate constant is for the ClO₄⁻ salt.

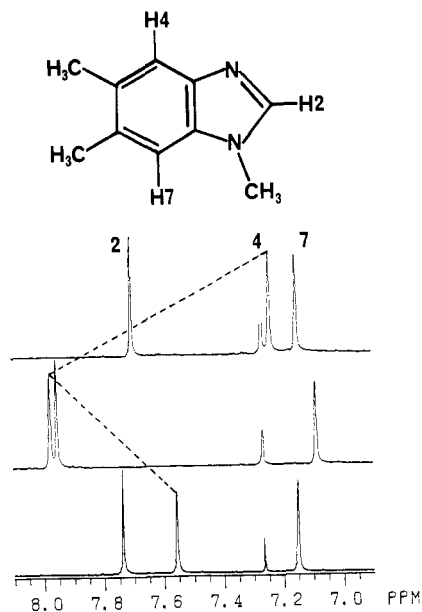


Figure 4. Me₃Bzm with labeling scheme and partial ¹H NMR spectra: (top) [Me₃BzmCo((DO)(DOH)pn)CH₃]ClO₄; (middle) Me₃BzmCo(DH)₂CH₃; (bottom) free Me₃Bzm. The signal at 7.26 ppm is CHCl₃. Solvent: CDCl₃.

Enhancement of L signals was not detected upon partial saturation of the more upfield multiplet. Hence, the upfield multiplet signal is assigned to the two N-CH₂ protons facing the alkyl side of the equatorial plane.

Discussion

A comparison of relevant geometric parameters for some Co(DH)₂ and Co(DO)(DOH)pn complexes is presented in Table X. The geometry of the axial fragment of I shows very small but significant differences from that of the analogous cobaloxime PhNH₂Co(DH)₂CH₃.²⁸ The two compounds have very similar Co-C bond lengths, but the Co-N distance of 2.129 (4) Å in PhNH₂Co(DH)₂CH₃ appears somewhat shorter than that of 2.147 (3) Å found in I. Compared with I, [pyCo((DO)(DOH)pn)CH₃]PF₆ shows again no significant change in the Co-C distance but does exhibit a decrease of the Co-N bond length to 2.106 (3) Å. Compared with I, pyCo(DH)₂CH₃ has the same Co-C bond length while the Co-N distance is shorter (2.068 (3) Å).

As expected, [PhNH₂Co((DO)(DOH)pn)CH₂CO₂CH₃]PF₆ (II) shows an increase of the Co-C length and a decrease of the Co-N distance with respect to I, since a carbomethoxymethyl group has larger bulk and is a poorer σ-donor than a methyl group (Table X). Comparison of II with pyCo(DH)₂CH₂CO₂CH₃ shows a trend similar to that observed in the comparison of the corresponding methyl derivatives. Thus, the Co-C bond length is unaffected by changing the equatorial ligand and is mainly influenced by the bulk of the alkyl group (steric cis influence).¹ In contrast, the Co-N axial bond is influenced by the nature of the equatorial ligand (electronic cis influence).²²

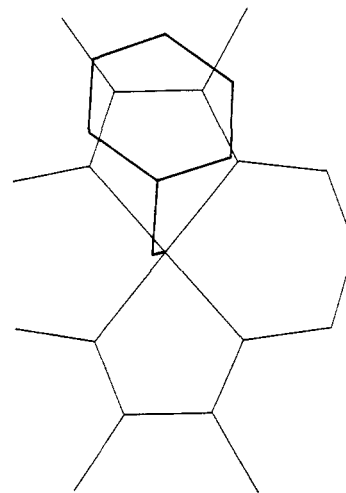


Figure 5. Orientation of aniline in I with respect to the equatorial moiety.

The data of Table X show that (DO)(DOH)pn complexes with PhNH₂ as the axial ligand have negative values of α (bending toward the neutral ligand), whereas the (DH)₂ complexes have small but positive α values. For example, the α bending of -11.3° in I is opposite to the bending of +3.5° found in the corresponding cobaloxime. The negative values of α for the (DO)(DOH)pn complexes containing PhNH₂ suggest that PhNH₂ is less bulky than py²⁶ and that the (DO)(DOH)pn equatorial ligand may be affected more strongly by the bulk of L than the (DH)₂ equatorial ligand. The orientation of PhNH₂ with respect to the equatorial moiety is very similar in I and II and is shown for I in Figure 5. Such an orientation is a common feature observed also in many PhNH₂Co(DH)₂R complexes with R = CH₃, CH₂CH₃, *i*-C₃H₇, CH₂OCH₃, CH₂C(CH₃)(COOEt)₂, and adamantyl,²⁹ and it may imply some attractive interaction between the phenyl group of PhNH₂ and the five-membered ring of the equatorial ligand. In contrast, the py ligand orientations are different by 90° in the complexes of the two systems.

The different orientation of the py ligand in the two series most probably arises from the steric effect of the propylene bridge. In the vicinity of Co, the PhNH₂ ligand is sterically smaller than py and such a steric effect may, in fact, be negligible. These structural features may be reflected in the trend in the rate constant values (Table X) in Co(DO)(DOH)pn and Co(DH)₂ methyl derivatives containing N-donor ligands. In the methyl cobaloximes, the rate constant for PhNH₂ is 190 times larger than that for py, in agreement with a longer Co-N distance (0.06 Å) for PhNH₂ relative to the py analogue. In the Co(DO)(DOH)pn complexes, this ratio is reduced to 15, corresponding to a decreased difference in the Co-N axial bond length (0.04 Å). This difference, in fact, may not be statistically significant (vide infra). Since the rate of displacement of a "small" ligand such as aniline may better represent the electronic nature of the cobalt center, we are led to the tentative conclusion that the cobalt center in the Costa-type model is more electrophilic than the cobalt center in cobaloximes. Therefore, the Costa models must be viewed as

(28) Mari, M. Ph.D. Thesis, University of Trieste, Italy.

(29) Randaccio, L., and co-workers, unpublished results.

relatively poor models of coenzyme B₁₂ and methyl B₁₂, which have relatively low electrophilicity for a Co(III) center.^{4,5,30}

On the other hand, for bulky ligands, particularly Me₃Bzm, the dissociation rates in Costa models exceed those for the analogous cobaloximes (Table IV). No structural comparisons for such Me₃Bzm compounds are possible, at this time. Insofar as the corrin ring of cobalamins is puckered,^{30,31} the bulk of the equatorial ligand in the Costa models and, perhaps, its flexibility appear to reflect more adequately the corrin ring system than does the planar, and perhaps more rigid, equatorial ligand system in cobaloximes.

The ligand 2NH₂py is very interesting in that, for cobaloximes, this ligand leads to weak Co-C bonds³² and to ambidentate behavior.^{3,33} However, of the binding sites (NH₂ or endocyclic py N), the endocyclic py N is usually greatly preferred as the binding site in cobaloximes.^{3,33} For the Costa system, such a coordination mode could be precluded by the puckered propylene bridge. Indeed, the data in Table IV are consistent with this analysis. Since amino-bound ligands are less reactive in the Costa system than those in cobaloximes, 2NH₂py should also be a slower leaving ligand if it were amino-bound in both systems. In fact, it is a slightly better leaving ligand in the Costa system. Similarly, although 2NH₂6Mepy is a very poor ligand compared to 2NH₂py in the cobaloxime system where 2NH₂6Mepy is clearly amino-bound,³³ 2NH₂py and 2NH₂6Mepy have essentially identical affinity for the Co((DO)(DOH)pn)CH₃ group. The relative affinities of L = 2NH₂6Mepy, 2NH₂py, and 2MeNHpy (2-methylaminopyridine) for Co((DO)(DOH)pn)CH₃ were determined by ¹H NMR observation of 1:1 equivalent mixtures of L with [PPh₃Co((DO)(DOH)pn)CH₃]ClO₄ in CD₂Cl₂. At equilibrium, 2NH₂py and 2NH₂6Mepy replaced 50% of PPh₃ while in the case of 2MeNHpy no replacement of PPh₃ occurred. Except for differences attributable to L, the ¹H NMR spectra of the products were nearly identical. For cobaloximes, 2NH₂py and 2MeNHpy have approximately the same affinity for Co(DH)₂R as assessed by ligand dissociation rates.³ This result is consistent with primarily endo N binding.

A more complete evaluation of the difference between the model systems requires extensive comparisons of activation parameters for the dissociation reactions. However, of the 16 L = N-donor complexes where comparisons are possible, the average value of the ratio of *k* for Co(DO)(DOH)pn to *k* for Co(DH)₂ is only 3.8 (Table IV).

These rate differences are relatively small and the differences could largely be a result of different ligand orientations. Unfortunately, suitable crystals have not yet been obtained for complexes with L other than py and PhNH₂. In any case, the orientation of the L group may be different in the solid and in solution. Since NMR methods have provided valuable information on the properties of cobaloximes in the past,¹ we thought that 1D NOE studies might be useful both in signal assignment and in gaining insight into ligand orientations.

¹H NMR chemical shifts of organocobalt compounds can be influenced by many factors.^{1,7,34} Three of the most important factors are (a) the anisotropy of Co, which generally induces upfield shifts of axial ligands and downfield shifts of the equatorial ligands as the electron-donor ability of the X or R group diminishes, (b) the ligand anisotropy with anisotropic axial ligands influencing the shifts of signals of equatorial ligand nuclei and vice versa, and (c), in contrast to the "through-space" effects a and b, a through-bond inductive effect also playing a role. Thus, the interpretation and assignment of NMR spectra can be complex unless the same solvent is employed and only one axial ligand is

Table XI. ¹H NMR Chemical Shifts for PhNH₂, py, LCo(DH)₂R, and [LCo((DO)(DOH)pn)R]ClO₄ (L = PhNH₂, py; R = CH₃, CH₂CO₂CH₃)^a

compd	chem shifts				
	α-H	β-H	γ-H	NH ₂	O-H...O
PhNH ₂	6.69	7.16	6.76	3.65	
PhNH ₂ Co(DH) ₂ CH ₃	6.64	7.18	7.05	4.14	18.14
[PhNH ₂ Co((DO)(DOH)pn)-CH ₃]ClO ₄	6.62	7.16	7.03	4.91	18.77
PhNH ₂ Co(DH) ₂ CH ₂ CO ₂ CH ₃ ^b	6.63	7.18	7.10	3.91	17.95
[PhNH ₂ Co((DO)(DOH)pn)-CH ₂ CO ₂ CH ₃]ClO ₄ ^b	6.59	7.13	7.08	4.77	18.52
py	8.61	7.29	7.68		
pyCo(DH) ₂ CH ₃	8.61	7.33	7.73		18.32
[pyCo((DO)(DOH)pn)CH ₃]ClO ₄	8.03	7.56	7.80		18.80
pyCo(DH) ₂ CH ₂ CO ₂ CH ₃	8.51	7.31	7.73		18.18
[pyCo((DO)(DOH)pn)-CH ₂ CO ₂ CH ₃]ClO ₄	7.87	7.55	7.78		18.46

^a Chemical shifts in ppm relative to internal Me₄Si (CDCl₃). ^b This complex is slightly soluble.

varied in a series. Even with such precautions, it may be difficult to "factor out" the electronic and anisotropic effects a and c. An additional problem is that the Co center is too heavy for simple theoretical calculations. Thus, the anisotropy is treated as adhering to a simple dipole model³⁴⁻³⁶—one which is particularly poor for interpreting shifts of nuclei close to the Co center.

If the equatorial ligand is maintained constant, the ¹H NMR shift of the Co-CH₃ resonance should reflect primarily the effects of a and c, above. Indeed, for cobaloximes and Costa models, as the electron-donor ability (basicity) of the py ligand is increased, 4CNpy < py < 4Me₂Npy, the Co-CH₃ signal moves upfield from 0.90 to 0.83 to 0.72 ppm for cobaloximes and 0.90 to 0.85 to 0.71 ppm for Costa compounds (Table VII). For anilines, the shift range is not as large in the series PhNH₂, MeOPhNH₂, and Me₂NPhNH₂, where the shifts change, respectively, from 0.81 to 0.78 to 0.77 ppm for cobaloximes and from 0.68 to 0.67 to 0.66 ppm for Costa compounds. The change in dissociation rates across these series is 220 (cobaloximes) and 870 (Costa) for the pyridines and 8.8 (cobaloximes) and 17 (Costa) for the anilines. Thus the affinity for Co of the anilines is not changing as greatly as that of the pyridines. However, in contrast to the pyridine ligands, where the shifts are similar for both systems (Δδ = 0.02 ppm), in the aniline series the Co-CH₃ shifts for the Costa compounds are at higher field (Δδ = 0.13 ppm). This comparison suggests but does not prove that less bulky aniline type ligands are relatively better electron donors in the Costa system than in the cobaloxime system. Consistent with this interpretation, the Co-CH₃ shifts for the Me₃Bzm compounds in the two series are similar. Likewise, for other bulky L, the equatorial CH₃ signal for cobaloximes is always upfield (ca. 0.14 ppm) from the oxime CH₃ signal in Costa compounds (Table VII). This difference is smaller for nonbulky L than for bulky L.

In a study of the effect of L on the Co-CH₃ chemical shifts in [4XpyCo((DO)(DOH)pn)CH₃]ClO₄ complexes,¹¹ it was concluded that transmission of the electronic effect of L through Co to CH₃ is highly efficient. The Co-CH₃ chemical shift moved 0.23 ppm upfield upon replacement of 4CNpy by 4NH₂py.¹¹

Pellizzer and co-workers have also observed movement of the Co-CH₃ signal to higher fields with increasing basicity of L.¹⁰ Replacement of the iodo ligand in ICo((DO)(DOH)pn)CH₃ moved the Co-CH₃ signal further upfield in the order *m*-FC₆H₄ < *p*-FC₆H₄ < C₆H₅ < CH₃.¹⁰ In another report, this group examined the ¹H NMR spectral trends which occurred upon addition of amino acids (and other N-donor ligands) to [H₂OCo((DO)(DOH)pn)CH₃]ClO₄.⁷ In contrast to the conclusions of other workers,¹¹ anisotropy of the L ligand, effect b, was cited as the major factor influencing the Co-CH₃ shift. It was found that ligands which bind through endocyclic nitrogen

(30) Rossi, M.; Glusker, J. P.; Randaccio, L.; Summers, M. F.; Toscano, P. J.; Marzilli, L. G. *J. Am. Chem. Soc.* **1985**, *107*, 1729.

(31) Glusker, J. P. In *B₁₂*; Dolphin, D., ed.; Wiley: New York, 1982, Vol. 1, p 23.

(32) Halpern, J. *Science (Washington, D.C.)* **1985**, *227*, 869 and personal communication.

(33) Marzilli, L. G.; Summers, M. F.; Zangrando, E.; Bresciani-Pahor, N.; Randaccio, L. *J. Am. Chem. Soc.*, in press.

(34) Trogler, W. C.; Stewart, R. C.; Epps, L. A.; Marzilli, L. G. *Inorg. Chem.* **1974**, *13*, 1564.

(35) McConnell, H. M. *J. Chem. Phys.* **1957**, *27*, 226.

(36) Brown, K. L.; Hakimi, J. M. *J. Am. Chem. Soc.* **1986**, *108*, 496.

Table XII. Chemical Shifts of ^{13}C NMR Resonances for py and PhNH_2 and Their $\text{LCo}(\text{DH})_2\text{R}$ and $[\text{LCo}(\text{DO})(\text{DOH})\text{pn}]\text{R}]\text{ClO}_4$ ($\text{R} = \text{CH}_3$, $\text{CH}_2\text{CO}_2\text{CH}_3$) Complexes^a

compd	chem shifts				
	$\alpha\text{-C}$	$\beta\text{-C}$	$\gamma\text{-C}$	$\text{O}-\text{N}=\text{C}$	$\text{O}-\text{N}=\text{C}-\text{CH}_3$
PhNH_2	115.12	129.31	118.59		
$\text{PhNH}_2\text{Co}(\text{DH})_2\text{CH}_3$	119.60	128.56	124.16	149.71	11.79
$[\text{PhNH}_2\text{Co}(\text{DO})(\text{DOH})\text{pn}]\text{CH}_3]\text{ClO}_4^b$	120.21	128.71	124.21	153.62	12.59
py	149.92	123.73	135.89		
$\text{pyCo}(\text{DH})_2\text{CH}_3$	150.06	125.21	137.48	148.98	11.98
$[\text{pyCo}(\text{DO})(\text{DOH})\text{pn}]\text{CH}_3]\text{ClO}_4^b$	148.77	126.76	138.73	153.71	12.92
$\text{pyCo}(\text{DH})_2\text{CH}_2\text{CO}_2\text{CH}_3^c$	150.23	125.39	137.97	150.79	12.38
$[\text{pyCo}(\text{DO})(\text{DOH})\text{pn}]\text{CH}_2\text{CO}_2\text{CH}_3]\text{ClO}_4^{b,c}$	148.85	127.09	139.17	155.51	13.35

^a Concentrations are 0.1 M except for that of $[\text{PhNH}_2\text{Co}(\text{DO})(\text{DOH})\text{pn}]\text{CH}_3]\text{ClO}_4$ which was 0.05 M. Chemical shifts are in ppm relative to internal Me_4Si in CDCl_3 . See ref 1 and 37 for further details. Aniline complexes with the $\text{CH}_2\text{CO}_2\text{CH}_3$ ligand have very poor solubility in CDCl_3 . The $\text{Co}-\text{C}$ and $\text{CH}_2^*\text{CO}_2\text{CH}_3$ signals were not observed. ^b The remaining shifts for the $\text{Co}(\text{DO})(\text{DOH})\text{pn}$ complexes are given as follows ($\text{PhNH}_2/\text{CH}_3$, py/CH_3 , $\text{py}/\text{CH}_2\text{CO}_2\text{CH}_3$): for $\text{C}-\text{N}=\text{C}$, 173.62, 173.56, 176.07; for $\text{C}-\text{N}=\text{C}-\text{CH}_3$, 17.08, 17.64, 18.20; for $\text{N}-\text{CH}_2-\text{CH}_2-\text{CH}_2-\text{N}$, 49.23, 49.50, 49.04; for $\text{N}-\text{CH}_2-\text{CH}_2-\text{CH}_2-\text{N}$, 27.36, 27.30, 27.06. ^c The shifts of the CO_2^*CH_3 signal are 50.98 and 51.30 ppm for the $(\text{DH})_2$ and $(\text{DO})(\text{DOH})\text{pn}$ complexes, respectively.

(e.g. histidine, py, NMeImd) cause lower field $\text{Co}-\text{CH}_3$ shifts and ligands which bind through exocyclic nitrogen (e.g. histidine pD9.5, phenylalanine) cause higher field $\text{Co}-\text{CH}_3$ shifts. It was felt that this difference was due to the different coordination geometries of L.⁷ The plane of py should be perpendicular to the equatorial plane while the plane of the imidazole ring of histidine would be more parallel to the equatorial plane. This explanation clearly is inadequate since complexes of both DEA and NH_3 , which lack anisotropic rings, exhibit the characteristic upfield shifts of the $\text{Co}-\text{CH}_3$ group (Table VII).

An interpretation of the $\text{O}-\text{H}\cdots\text{O}$ signal in these systems as a function of L is complicated because this signal will be further downfield when the H bonding is strongest.¹ The consistently further downfield shift of the Costa compound vs. that of the analogous cobaloxime compound probably reflects the stronger H bonding (shorter $\text{O}\cdots\text{O}$ distance) in the Costa model systems (Table VII).¹²

The $\alpha\text{-H}$ shift of pyridine-type ligands is believed to be highly sensitive to Co anisotropy in the cobaloxime series.³⁴ The $\alpha\text{-H}$'s most probably lie over the $\text{Co}-\text{N}-\text{O}\cdots\text{H}-\text{O}-\text{N}$ chelate rings¹ and are not greatly subject to the anisotropy of the $\text{Co}-\text{N}=\text{C}-\text{C}=\text{N}$ rings (effect b). The $\alpha\text{-H}$ shift of py is very little affected by coordination to $\text{Co}(\text{DH})_2\text{CH}_3$ (Table IX). In contrast, the $\alpha\text{-H}$ shift is greatly influenced (ca. 0.6 ppm upfield shift) by coordination to $\text{Co}(\text{DO})(\text{DOH})\text{pn}]\text{CH}_3$ (Table VIII).¹⁰ This difference could be due to any one of or a combination of a-c above.

The least probable factor is c. The cobalt center in Costa compounds is likely to be less electron rich than in cobaloximes; this situation should lead to a *downfield* shift of the $\alpha\text{-H}$ signal. Instead, an upfield shift is observed. The Co center could be more anisotropic in these $\text{Co}-\text{CH}_3$ compounds for the Costa system than for the cobaloximes. If this were the case, the $\text{Co}-\text{CH}_3$ signal might be at higher fields—but the shifts of this signal in the pyridine series are similar (Table VII). So greater anisotropy alone is not an adequate explanation for the shift of the $\text{Co}-\text{CH}_3$ signal.

On the other hand, if the Costa cobalt center is less electron rich but more anisotropic, the results can be understood. Anisotropy would lead to upfield shifts of axial ligands and electron deficiency to downfield shifts. The shift of the $\alpha\text{-H}$ of pyridines is not very sensitive to inductive effects (effect c) and hence the "electronic richness" of Co.³⁴ Thus, anisotropy (effect a) will dominate. The $\text{Co}-\text{CH}_3$ shift may be more sensitive to electronic richness and, on balance, could have a similar shift in the two series.

Several aspects of our ^1H NMR data appear consistent with this counteracting effect hypothesis. For example, the NH signals of amine ligands are further downfield (ca. 0.7 ppm) for Costa compounds than for cobaloximes (Table VIII). Perhaps "electronic richness" effects dominate over anisotropy for NH signals. Likewise, because of the $1/R^3$ dependence of anisotropy,³⁵ signals of nuclei remote from cobalt but conjugated to the ligand-donor atom (such as the $\beta\text{-H}$ of py, H7 of Me_3Bzm) will

reflect primarily "electronic richness". These signals of compounds with such L are relatively *downfield* (Tables VIII and IX) for Costa-type compounds.

The NMeImd comparison is interesting. The H4 signal of NMeImd behaves in the two series like the $\alpha\text{-H}$ for the py analogues. However the H2 signal (H2 should be in a sterically equivalent position to H4) is downfield for the Costa compound relative to the cobaloxime. This downfield shift could be due to a reorientation (by 90°) of the plane of the smaller NMeImd ring relative to that of the pyridine ring. However, the H4 signal should then also be relatively downfield. Instead, it is still upfield. We believe that the H2 signal of NMeImd is perhaps more sensitive to through bond effects than are either the signals of the H4 or the py $\alpha\text{-H}$ protons. The N1- CH_3 and H5 signals are downfield in the Costa model relative to the cobaloxime. This result is also consistent with a greater withdrawal of electron density from the axial ligand by Co in the Costa-type model.

From Table XI, the effect of changing the alkyl group from CH_3 to $\text{CH}_2\text{CO}_2\text{CH}_3$ on the ^1H NMR signals of L (PhNH_2 and py) is seen. The effects of anisotropy (a and b) and induction (c) are clearly evident. Signals for nuclei remote from the Co (primarily influenced by induction) are shifted downfield in going from the CH_3 to the $\text{CH}_2\text{CO}_2\text{CH}_3$ analogue (e.g. those for py $\gamma\text{-H}$, py $\beta\text{-H}$, and PhNH_2 $\gamma\text{-H}$). Shorter $\text{Co}-\text{N}$ bond lengths in the $\text{CH}_2\text{CO}_2\text{CH}_3$ analogues should lead to a greater influence of Co anisotropy on the L signals. Indeed, signals for nuclei close to Co (py $\alpha\text{-H}$, PhNH_2 , NH_2) are upfield in the $\text{CH}_2\text{CO}_2\text{CH}_3$ compounds.

Limited ^{13}C NMR studies were carried out on the pyridine compounds (Table XII). With respect to the free ligand, the $\alpha\text{-C}$ signal moves upfield for Costa compounds but downfield for cobaloximes. The $\beta\text{-C}$ and $\gamma\text{-C}$ signals, which are more likely to reflect Co electrophilicity,^{1,37} are downfield for the Costa compounds, in agreement with our interpretation that the Co center is relatively electron poor. These latter C atoms as well as the PhNH_2 C atoms with observable signals (Table XII) are remote from the Co and their shifts will reflect inductive effects. A comparison of results for $\text{Co}-\text{CH}_3$ and $\text{Co}-\text{CH}_2\text{CO}_2\text{CH}_3$ compounds in Table XII supports this analysis since $\text{CH}_2\text{CO}_2\text{CH}_3$ is a poorer electron donor than CH_3 . This relative electron-donor ability of the R groups is also evident in shifts of the C signals of the equatorial ligands. It should be noted that such shifts cannot be compared between systems because of the different equatorial ligands. Also, only limited ^{13}C NMR studies have been carried out with Costa type compounds.

We may well ask: Is the greater anisotropy of $\text{Co}(\text{DO})(\text{DOH})\text{pn}]\text{CH}_3^+$ compared to $\text{Co}(\text{DH})_2\text{CH}_3$ based on the Co or on the equatorial ligand? Pellizer and co-workers have suggested that the effect is due to the ligand.⁷ If the effect is equatorial-ligand-based, the greater anisotropy of $(\text{DO})(\text{DOH})\text{pn}$ compared

to (DH)₂ should be in the vicinity of the Schiff base double bonds. The Me₃Bzm compound is of some interest in this connection. The H4 signal is 0.74 ppm further upfield for the Costa model than for the (DH)₂ complex (Figure 4, Table VIII). The H4 nucleus should lie out over the double bonds of the equatorial ligands. The 1D NOE data clearly show that the propylene protons are not near the H4 proton of coordinated Me₃Bzm. In contrast, the H2 signal is enhanced by irradiation of propylene N-CH₂ protons lying on the L side of the equatorial plane. Indeed, the α-H signals of the PhNH₂ and py compounds also gave an NOE with the most downfield multiplet assigned to these CH₂ groups of the propylene bridge. These results suggest that the L ligand is rotating relatively freely. Clearly, more studies are needed to (i) resolve the issue of the reasons for the greater anisotropy of the Co((DO)(DOH)pn)CH₃⁺ group compared to the Co(DH)₂CH₃ group and (ii) assess the relative contributions of effects a and b to the shifts of the axial ligand signals.

The above NOE studies suggest that the downfield multiplet in all cases is assignable to the H's on the terminal CH₂ groups of the propylene bridge which lie on the L side of the equatorial plane. Indeed, when L is an aniline type ligand, this multiplet is relatively upfield (3.8 to 3.9 ppm). The multiplet of most of the complexes in Table VII appears at ca. 4.0 ppm or to even lower field. This observation is consistent with the effect of the anisotropic ring of the aniline-type ligands. The 2NH₂py compound follows the trend, and this result supports NH₂ binding by this ligand. Likewise, the shifts of the equatorial CH₃ groups are ca. 0.2 ppm more upfield than for most other compounds in Table VIII for both the aniline-type ligands and 2NH₂py—again, consistent with NH₂ binding in the Costa system.

In conclusion, our extensive comparison of the [LCo((DO)(DOH)pn)CH₃]X and LCo(DH)₂CH₃ compounds for L = N-

donor ligand does not indicate any major differences in structure or properties comparable in magnitude to those found between these systems and cobalamins on the one hand and Schiff base models such as Cosaloph compounds on the other hand. Clearly, compared to cobaloximes, steric effects are more important in the Costa-type models, which also exhibit greater anisotropy. The basis for the anisotropic effect is still uncertain but it seems clear that the Co center in the Costa-type models is more electrophilic than that of the cobaloxime. Since the Co center in cobalamins has relatively low electrophilicity for a Co compound, the Costa-type models are clearly deficient. On the other hand, Co-N-(axial) bond lengths are somewhat longer for Costa type compounds—a result more in keeping with cobalamin structures.^{30,31} Although comparable to cobaloximes, the lower symmetry of the Costa-type compounds leads to more complex NMR spectra, the very complexity of the spectra eventually could be useful in evaluating the various contributions of a-c in influencing NMR shifts. In turn, such information could prove useful in interpreting the relationship of NMR spectra of cobalamins to their conformation—a subject of vital importance in unraveling B₁₂-dependent enzymatic processes.^{30,36}

Acknowledgment. This research was supported by NIH Grant GM29225 to L.G.M. and by a grant from the MPI (Rome) to L.R. The purchase of the 360-MHz NMR instrument was supported in part by an NSF departmental grant to Emory. We are grateful to these organizations. The research was also supported, in part, by an Emory Research Grant.

Supplementary Material Available: Tables of elemental analyses, anisotropic thermal parameters, hydrogen atom coordinates, and complete bond lengths and bond angles (12 pages). Ordering information is given on any current masthead page.

Contribution from the Institut de Recherches sur la Catalyse, CNRS conventionné à l'Université Claude Bernard, 69626 Villeurbanne Cédex, France, and Laboratoire d'Etudes Dynamique et Structurale de la Sélectivité, UA 332 CNRS, 38402 Saint Martin d'Hères Cédex, France

Cationic Metal Nitrosyl Complexes. 6. Characterization of the 19-Electron Radical Cation [Fe(NO)₂LL'₂]⁺

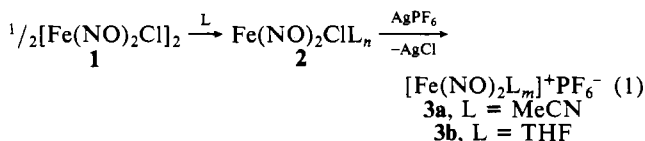
D. Ballivet-Tkatchenko,^{*1a} B. Nickel,^{1b} A. Rassat,^{1b} and J. Vincent-Vaucouelin^{1a}

Received February 20, 1986

The reaction of [Fe(NO)₂Cl]₂ with AgPF₆ in THF or MeCN leads to the formation of a radical cation that initiates the cationic polymerization of activated olefins. On the bases of ESR and IR experiments in the presence of PPh₃, P(OPh)₃, *trans*-PPh₂-(CH=CH)PPh₂, or PPh₂CH₂CH₂PPh₂, the radical cation corresponds to the 19-electron complex [Fe(NO)₂LL'₂]⁺ in a trigonal-bipyramidal arrangement with two equivalent NO and L ligands in the equatorial plane (L = L' = THF, MeCN, PPh₃; L = PPh₃, L' = THF, MeCN). EHMO calculations agree with the ESR features. This five-coordination (19-electron configuration) is relevant to the electrophilic behavior of the iron ion, which is induced by the presence of the cationic charge and of the two NO ligands.

The structure determinations of mononuclear metal-nitrosyl complexes have shown that the M-N-O bond angles vary in the range 180–120°.² Conversion of linear into bent NO is a feasible process³ and corresponds formally to the withdrawal of two electrons from the metal. Such a situation generates coordinatively unsaturated metal centers, a prerequisite for catalysis. In this context our interest has been focused toward the catalytic properties of [Fe(NO)₂Cl]₂ (1). Vinyl compounds are polymerized when a cocatalyst such as AgPF₆ (BF₄ or ClO₄) is added to a

solution of 1.⁴ The conversion is optimum for Fe:Ag = 1, and AgCl quantitatively precipitates. These observations suggest that Cl⁻-PF₆⁻ (BF₄⁻, ClO₄⁻) anion exchange has occurred, leaving in solution the solvated cationic complex 3 (eq 1) acting as the



initiator for the polymerization at low temperature (≤25 °C).

- (1) (a) Institut de Catalyse. Present address: CNRS-LCC, 205 route de Narbonne, 31400 Toulouse, France. (b) UA 332.
(2) Feltham, R. D.; Enemark, J. H. *Top. Stereochem.* **1981**, *12*, 155–215.
(3) Collman, J. P.; Farnham, P.; Dolcetti, G. *J. Am. Chem. Soc.* **1971**, *93*, 1788–1790.

- (4) Ballivet-Tkatchenko, D.; Billard, C.; Revillon, A. *J. Polym. Sci., Polym. Chem. Ed.* **1981**, *19*, 1697–1706.